Turk J Chem
33 (2009) , 599 – 606.

doi:10.3906/kim-0812-22

Hydrogen storage via physisorption: the combined role of adsorption enthalpy and entropy

Carlos Otero AREAN[1,*], Barbara BONELLI[2], Montserrat Rodriguez DELGADO[1], Edoardo GARRONE[2]

[1] *Department of Chemistry, University of the Balearic Islands, Palma de Mallorca-SPAIN*
e-mail: dqueep0@uib.es

[2] *Department of Materials Science and Chemical Engineering, Polytechnic of Torino, Turin-ITALY*

Received 05.12.2008

Materials capable of cost-effective on-board hydrogen storage and delivery are currently being sought worldwide as a means to facilitate a hydrogen-based energy transition in the transportation sector. Among the solutions proposed, hydrogen storage by physisorption on porous solids constitutes a main avenue of research, and for intelligent design of such materials a detailed knowledge of gas adsorption thermodynamics is of the utmost importance. Analysis of the available data for hydrogen adsorption on alkali and alkaline-earth cation exchanged zeolites clearly shows that standard adsorption enthalpy (ΔH^0) and entropy (ΔS^0) are correlated, in the sense that larger ΔS^0 values correspond to larger ΔH^0 values. It was also shown that, referring to absolute values, the relative rate at which adsorption entropy changes decreases gradually as adsorption enthalpy increases thus resulting in a non-linear correlation between ΔH^0 and ΔS^0. These results are discussed and corresponding implications for hydrogen storage via physisorption are highlighted.

Key Words: Adsorption thermodynamics; enthalpy-entropy correlation; hydrogen physisorption; hydrogen storage.

Introduction

The proposed use of hydrogen as an energy carrier (fuel) that could help overcome environmental and economic problems in the transportation sector is contingent upon solving the problem of cost-effective on-board hydrogen

*Corresponding author

storage and transport.[1–3] At present, most prototype hydrogen powered vehicles use either gas cylinders in which hydrogen is compressed at a high pressure (typically 300-350 bar) or liquid hydrogen cryogenic tanks;[2,4] however, neither of these solutions is free of demanding technical complexities. As such, intensive research is underway worldwide in the attempt to find materials with adequate capacity for hydrogen storage and delivery, preferably at (or near) ambient temperature and moderate pressure. Among the solutions being sought, hydrogen storage via molecular adsorption (physisorption) on low density porous solids constitutes a main avenue of research.

Light hydrogen adsorbents currently under research include porous carbons, organic polymers with intrinsic microporosity (PIMs), and porous metal-organic frameworks (MOFs).[2] As physisorption is a non-activated process, reversible and fast hydrogen uptake and delivery can be expected, constituting a major advantage of porous adsorbents over metal hydrides, which constitute another kind of material proposed for hydrogen storage and transport.[1,2] Nonetheless, the disadvantage of hydrogen physisorbents is that gas-solid interaction energy is usually low, and hence, significant hydrogen storage only takes place at low temperatures or exceedingly high pressures.[5–9] Therefore, in the quest for enhanced hydrogen storage, a primary aim is to tailor porous adsorbents to obtain materials with higher adsorption energy for hydrogen.

Thermodynamic constraints for hydrogen storage via physisorption were analyzed by Bhatia and Myers,[10] with a focus on porous carbons. Assuming Langmuir-type adsorption, they derived the equation

$$\Delta H^0_{opt} = T\Delta S^0 + [(RT/2)ln(P_1P_2/P_0^2)] \quad (1)$$

in which the optimum value of adsorption enthalpy (ΔH^0_{opt}) for hydrogen delivery is a function of temperature (T) and adsorption entropy (ΔS^0), P_0 is the standard pressure value to which ΔS^0 is referred, P_1 is the hydrogen loading pressure, and P_2 is the exhaust delivery pressure. Alternatively, the optimum operational temperature for hydrogen storage-delivery cycles between pressure P_1 and P_2 is given below:

$$T_{opt} = \Delta H^0/[\Delta S^0 + (R/2)ln(P_1P_2/P_0^2)] \quad (2)$$

It should be noted, however, that practical use of the above equations requires knowledge of the actual entropy change involved in the hydrogen adsorption process, which, in general terms, cannot be assumed to be independent of enthalpy change, as shown by recent studies on the thermodynamics of hydrogen adsorption on several cation-exchanged zeolites.[11–13] Available data for these materials were analyzed with 2 primary aims in mind: first, to show how the entire set of data for hydrogen adsorption on zeolites clearly proves that a strong correlation exists between adsorption enthalpy and entropy and, secondly, to highlight the implications of such a correlation in the search for suitable hydrogen adsorbents for on-board hydrogen storage and delivery.

Zeolites as model systems for hydrogen adsorption

The high density of the aluminosilicate framework renders zeolites unlikely candidates for hydrogen storage, as their maximum hydrogen uptake (about 3% by weight)[14] is far from the established target of 6-9 wt% for on-board hydrogen storage systems.[2,15] Yet, a well-defined crystal structure and easy ion exchange make zeolites ideal porous adsorbents for systematic studies of hydrogen binding to a large variety of metal cation centers, and such studies should facilitate data useful for designing (more prospective) lighter adsorbents, such as MOFs

and related materials. By using variable-temperature infrared (VTIR) spectroscopy[11,16] the thermodynamics of hydrogen adsorption on several alkali[11,17,18] and alkaline-earth[13,19,20] cation-exchanged zeolites was studied. The basis and experimental details of the method used can be found elsewhere,[11,16] but a brief outline is given below in order to facilitate understanding of the relevant results.

Localized adsorption of hydrogen molecules on the extra-framework (exchangeable) cations of zeolites leads to activation in the infrared of the fundamental H–H stretching mode, which shows the characteristic IR absorption band red-shifted from the wavenumber value of the corresponding (Raman active) mode of gas-phase molecular hydrogen.[21–23] At any given temperature the integrated intensity of the characteristic IR absorption band should be proportional to surface coverage (θ), thus providing information on the activity of both the adsorbed species and the empty adsorption sites (1-θ); simultaneously, the equilibrium pressure indicates the activity of the gas phase. Hence, the corresponding adsorption equilibrium constant (K) can be determined and the variation of K with temperature gives the corresponding values of adsorption enthalpy and entropy. Integrated band intensity (A), temperature (T), and equilibrium pressure (p), determined simultaneously by using an appropriate (variable-temperature) IR cell,[24] are considered to be inter-related by the Langmuir-type equation:

$$\theta = A/A_M = K(T)p/[1 + K(T)p] \tag{3}$$

where A_M is the integrated band intensity corresponding to full coverage ($\theta = 1$). Combining Eq. (3) with the van't Hoff Eq. (4) leads to Eq. (5) below:

$$K(T) = \exp[-\Delta H^0/RT] \exp[\Delta S^0/R] \tag{4}$$

$$\ln[A/(A_M - A)p] = (-\Delta H^0/RT) + (\Delta S^0/R) \tag{5}$$

By plotting the left-hand side of Eq. (5) against the reciprocal of the temperature, for measurements obtained over a relatively large temperature range, corresponding values of adsorption enthalpy (ΔH^0) and entropy (ΔS^0) are directly obtained, as shown in Figure 1 for hydrogen adsorption on the zeolite Li-FER[18] (which is reproduced here as an example of how the VTIR method is applied). Reported results for Li-FER and several other zeolites are summarized in the Table. It should be noted that original ΔS^0 values referred to a standard state at 1 Torr (1.33 mbar) and 100 K, representative of the pressure and temperature range at which IR spectra were obtained. Within the perfect gas approximation, ΔS^0 values referred to a standard pressure of 1 bar can be obtained by adding 55 J mol^{-1} K^{-1} to the corresponding values reported in the Table. Note that this change of reference state would not have any effect on ΔH^0.

Enthalpy-entropy correlation

Data reported in the Table clearly show that both standard adsorption enthalpy and entropy depend on the adsorbent (zeolite) being considered. They also show a clear (positive) correlation between adsorption enthalpy and entropy; referring to absolute values, ΔS^0 is observed to increase when ΔH^0 increases. The reasons for this experimentally observed correlation and corresponding implications for hydrogen storage via physisorption are discussed below; however, we shall first look more closely at the mode in which ΔH^0 and ΔS^0 are correlated.

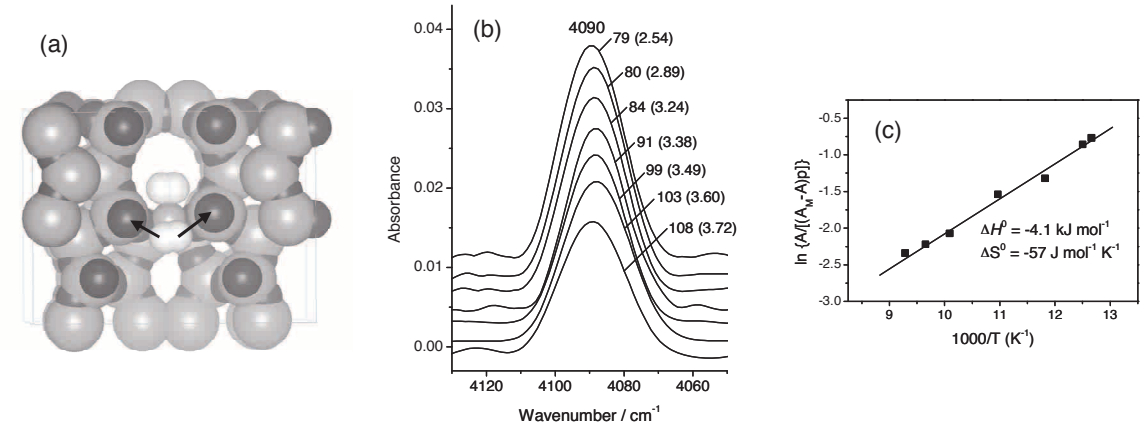

Figure 1. (a) Two hydrogen molecules can be adsorbed (with approximately the same interaction energy) on a Li^+ ion in the zeolite Li-FER. Note, however, that there is a small destabilization of the adsorption complex because of the interaction between the zeolite framework and nearby oxygen atoms (marked with arrows). Further details can be found in reference 18. (b) Representative variable-temperature IR spectra of hydrogen adsorbed on Li-FER. Temperature (K) and pressure in Torr (between brackets) are shown. (c) Plot of the left-hand side of Eq. (5) as a function of reciprocal temperature for determining adsorption enthalpy and entropy.

Table. Spectroscopic and thermodynamic data for hydrogen adsorbed on several zeolites. Error limits for ΔH^0 and ΔS^0 are $\pm$ 1 kJ mol^{-1} and $\pm$ 10 J mol^{-1} K^{-1}, respectively.[a]

Zeolite	ν(H–H) cm^{-1}	ΔH^0 kJ mol^{-1}	$\Delta S^{0,b}$ J mol^{-1} K^{-1}	Ref.
Li-FER	4090	−4.1	−57	18
Na-FER	4100	−6.0	−78	11,36
K-FER	4111	−3.5	−57	11,36
Li-ZSM-5	4092	−6.5	−90	11
Na-ZSM-5	4101	−10.3	−116	11
Mg-X	4066	−11	−105	12
(Mg,Na)-Y	4056	−18	−136	19,20
Ca-Y	4078	−15	−127	13

[a] ΔH^0 and ΔS^0 values are given per mole of molecular hydrogen.

[b] Referred to a standard state at 1 Torr (1.33 mbar).

For that purpose, ΔH^0 values are plotted against corresponding ΔS^0 values in Figure 2. Clearly, the observed correlation is not linear. The increasingly sloping curve that was obtained shows that (referring to absolute values) the relative rate at which adsorption entropy changes decreases gradually as adsorption enthalpy increases. Similar results regarding several chemical processes driven by weak interaction forces, for which a positive enthalpy-entropy correlation (also termed entropy-enthalpy compensation) was often observed to occur, have been reported. Examples include formation of weakly associated molecular complexes,[25,26] hydrogen bonding,[27] Langmuir-type adsorption from solution,[28] and heterogeneous catalysis.[29] When ΔH^0

and ΔS^0 values cover only a small temperature range linear correlations are sometimes obtained,[11,30,31] but curves similar to that shown in Figure 2 were frequently reported.[25,30,32]

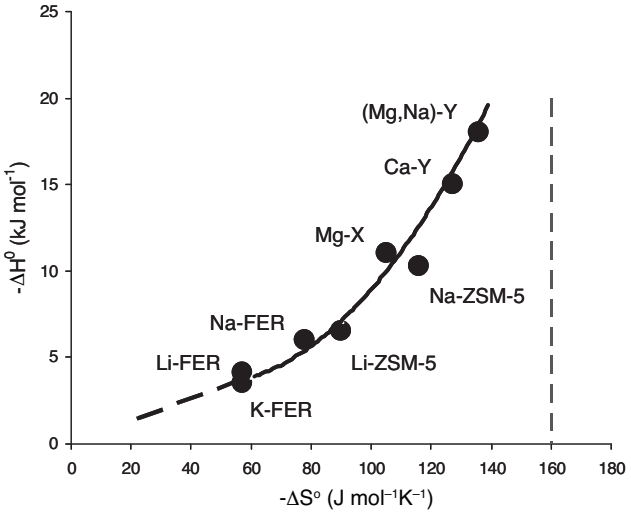

Figure 2. Standard adsorption enthalpy versus entropy for hydrogen adsorption on several cation-exchanged zeolites. Note that a similar correlation, not including Li-FER, can be found in reference 12.

Discussion and conclusions

Polarization of the hydrogen molecule by the cationic adsorbing centers is known to be the main factor accounting for hydrogen adsorption on alkali and alkaline-earth cation exchanged zeolites.[33–35] Theoretical calculations have shown that the hydrogen molecule interacts side-on with zeolite (extra-framework) cations, forming a T-shaped adsorption complex,[11,33,36] as shown in Figure 1a. This interaction renders the H–H stretching mode active in the IR and results in a bathochromic shift from the corresponding Raman-active mode (at 4163 cm^{-1}) of the free molecule. In principle such a red-shift should correlate with the polarizing power of the cation involved and the same should hold for the corresponding interaction energy. In fact, the data shown in the Table follow this general trend, but there are some exceptions. For instance, the enthalpy of hydrogen adsorption on Li-FER and Li-ZSM-5 is less than the corresponding ΔH^0 value for Na-FER and Na-ZSM-5, respectively, despite Li^+ being a more polarizing cation than Na^+. Detailed theoretical calculations, at the periodic DFT level,[11,18] have shown that these exceptions can be accounted for when residual interactions of the adsorbed hydrogen molecule with nearby oxygen anions of the zeolite framework are also taken into consideration. These residual interactions can destabilize the adsorption complex to a greater extent when a very small cation (Li^+) is involved; due to the closer proximity of framework anions.

Regarding the thermodynamics of the hydrogen adsorption process, the observed correlation between adsorption enthalpy and entropy is likely to be because a stronger (enthalpy related) interaction between hydrogen molecules and the zeolite adsorbing centers results in a larger decrease of motion freedom of such molecules, and hence in a greater (entropy related) order of the system. In more precise terms, it should be noted that adsorbed hydrogen molecules still have some rotational freedom, as shown by IR spectroscopy

of combination modes;[21] however, adsorption results in the loss of translational motion and the simultaneous appearance of intermolecular vibrational modes, i.e. vibration of the adsorbed molecule against the binding site. Higher interaction energy, and consequently larger enthalpy change, will necessarily lead to a higher frequency of intermolecular vibration modes and hence to a greater entropy change. This argument is strongly supported by the results of recent studies[37,38] on hydrogen adsorption on Na^+, Ca^{2+}, and Zn^{2+} exchanged faujasite-type zeolites by means of inelastic neutron scattering (INS). The frequency of the intermolecular vibrational mode, which appeared in the low energy region of the INS spectra, was directly proportional to the polarizing power of the cation involved ($Na^+ < Ca^{2+} < Zn^{2+}$), which, as already pointed out above, is the main factor contributing to the cation-hydrogen interaction energy.

It should be noted that the adsorption enthalpy, which reflects the magnitude of the interaction energy between the hydrogen molecule and the adsorbing center, does not have (in principle) any defined upper limit. Yet, since the adsorbed molecules cannot lose more than all of their degrees of translation and rotational freedom, the adsorption entropy does have a limit. Such a limit in ΔS^0 (applicable to the data plotted in Figure 2) is the entropy content of 1 mol of hydrogen at 1 Torr and 100 K, which, following standard thermodynamic calculations, is -179 J mol^{-1} K^{-1}. Nonetheless, as previously mentioned, the adsorbed state still has some rotovibrational entropy content and, therefore, the actual maximum value of ΔS^0 less (in absolute value) than -179 J mol^{-1} K^{-1}; the plot in Figure 2 suggests that a value of about -160 J mol^{-1} K^{-1} (vertical dotted line) should be a reasonable estimate.

The correlation between adsorption enthalpy and entropy has important consequences for hydrogen storage in porous adsorbents. A main point to bear in mind is that, for an optimum storage-delivery cycle, the absolute value of adsorption enthalpy should be neither too high nor too low. Too high an adsorption enthalpy would impair performance, because a large amount of hydrogen would be retained by the adsorbent at the exhaustion pressure, whereas if ΔH^0 is too low the adsorbent would have only a very small capacity for hydrogen storage at ambient temperature and reasonable pressure.

The case of low adsorption enthalpy can be typified by porous carbons and other adsorbents that mainly show dispersion-type interaction forces with adsorbed hydrogen. Assuming $P_1 = 30$ bar and $P_2 = 1.5$ bar are reasonable pressure values for the hydrogen storage-delivery cycle, and taking $\Delta S^0 = -66.5$ J $mol^{-1}{\cdot}K^{-1}$ as a representative value of adsorption entropy change for hydrogen on carbons[10] Eq. (1) yields $\Delta H^0_{opt} = -15.1$ kJ mol^{-1} at 298 K. Yet, typical ΔH^0 values reported for carbons[10,39] range from -5 to -8 kJ mol^{-1}; hence, useful hydrogen storage via physisorption on these materials can only be attained at a cryogenic temperature.[10,40,41] A second major class of hydrogen adsorbents is typified by MOFs and related materials. In contrast to carbons, many MOFs possess coordinatively unsaturated metal cations (open-metal sites), which, similarly to those in zeolites, can act as polarizing centers for (localized) hydrogen adsorption.[42–47] In such a case, adsorption enthalpy could be significantly greater than that for carbons and related materials, as shown by the data in the Table; however, because of the enthalpy-entropy correlation, adsorption entropy is also expected to be greater than for carbons and, therefore, ΔH^0_{opt} (as derived from Eq. (1)) would be significantly greater than -15.1 kJ mol^{-1}. In fact, extrapolation of the data in the Table and Figure 2 suggests an optimum enthalpy value[2] of about -25 kJ mol^{-1}, and this is another important point to bear in mind when designing prospective hydrogen adsorbents. Finally, a third relevant consideration involves pore size. Larger pores would certainly increase hydrogen uptake, but what is most important is excess capacity,[2] meaning how much hydrogen can be stored

in a pore volume that would not be stored (at the same temperature and pressure) in a standard container, i.e. a gas cylinder. Excess capacity implies tighter packing of hydrogen molecules, which can only be obtained with increased interaction energy. Because this energy is maximized when there is direct contact between adsorbed molecules and polarizing adsorption centers, what would work best is a large microporous volume made of narrow pores with large surface density of open-metal sites. Ideally, the optimum pore diameter is likely to be not much larger than twice the kinetic diameter of the hydrogen molecule (2.9 Å); as that would lead to tighter packing of gas molecules in the adsorbed state.

References

1. Züttel, A. *Mater. Today* **2003**, *6*, 24-33.
2. van den Berg, A. W. C.; Arean, C. O. *Chem. Commun.* **2008**, 668-681.
3. Balat, M. *Int. J. Hydrogen Energy* **2008**, *33*, 4013-4019.
4. von Helmolt, R.; Eberle, U. *J. Power Sources* **2007**, *165*, 833-843.
5. Rosi, N. L.; Eckert, J.; Eddaoudi, M.; Vodak, D. T.; Kim, J.; O'Keeffe, M.; Yaghi, O. M. *Science* **2003**, *300*, 1127-1129.
6. Schimmel, H. G.; Kearly, G. J.; Nijkamp, M. G.; Visser, C. T.; de Jong, K. P.; Mulder, F. M. *Chem. Eur. J.* **2003**, *9*, 4764-4770.
7. Collins, D. J.; Zhou, H. C. *J. Mater. Chem.* **2007**, *17*, 3154-3160.
8. Mulder, F. M.; Dingemans, T. J.; Schimmel, H. G.; Ramirez-Cuesta, A. J.; Kearly, G. J. *Chem. Phys.* **2008**, *351*, 72-76.
9. Thomas, K. M. *Catal. Today* **2007**, *120*, 389-398.
10. Bhatia, S. K.; Myers, A. L. *Langmuir* **2006**, *22*, 1688-1700.
11. Otero Arean, C.; Nachtigallova, D.; Nachtigall, P.; Garrone, E.; Rodriguez Delgado, M. *Phys. Chem. Chem. Phys.* **2007**, *9*, 1421-1437.
12. Garrone, E.; Bonelli, B.; Otero Arean, C. *Chem. Phys. Lett.* **2008**, *456*, 68-70.
13. Turnes Palomino, G.; Llop Carayol, M. R.; Otero Arean, C. *Catal. Today* **2008**, *138*, 249-252.
14. Vitillo, J. G.; Ricchirardi, G.; Spoto, G.; Zecchina, A. *Phys. Chem. Chem. Phys.* **2005**, *7*, 3948-3954.
15. Read, C.; Thomas, G.; Ordaz, G.; Satyapal, S. *Mater. Matters* **2007**, *2*, 3-4.
16. Garrone, E.; Otero Arean, C. *Chem Soc. Rev.* **2005**, *34*, 846-857.
17. Otero Arean, C.; Manoilova, O.V.; Bonelli, B.; Rodriguez Delgado, M.; Turnes Palomino, G.; Garrone, E. *Chem. Phys. Lett.* **2003**, *370*, 631-635.
18. Nachtigall, P.; Garrone, E.; Turnes Palomino, G.; Rodriguez Delgado, M.; Nachtigallova, D.; Otero Arean, C. *Phys. Chem. Chem. Phys.* **2006**, *8*, 2286-2292.
19. Turnes Palomino, G.; Llop Carayol, M. R.; Otero Arean, C. *J. Mater. Chem.* **2006**, *16*, 2884-2885.
20. Otero Arean, C.; Turnes Palomino, G.; Llop Carayol, M. R. *Appl. Surf. Sci.* **2007**, *253*, 5705-5708.
21. Kazansky, V. B. *J. Mol. Catal. A* **1999**, *141*, 83-94.

22. Solans-Monfort, X.; Branchadell, V.; Sodupe, M.; Zicovich-Wilson, C. M.; Gribov, E.; Spoto, G.; Busco, C.; Ugliengo, P. *J. Phys. Chem. B* **2004**, *108*, 8278-8286.
23. Bordiga, S.; Garrone, E.; Lamberti, C.; Zecchina, A.; Otero Arean, C.; Kazansky, V. B.; Kustov, L. M. *J. Chem. Soc. Faraday Trans.* **1994**, *90*, 3367-3372.
24. Tsyganenko, A. A.; Storozhev, P. Y.; Otero Arean, C. *Kinet. Catal.* **2004**, *45*, 530-540.
25. Westwell, M. S.; Searle, M. S.; Klein, J.; Williams, D. H. *J. Phys. Chem.* **1996**, *100*, 16000-16001.
26. Stolov, A. A.; Herrebout, W. A.; van der Veken, B. J. *J. Am. Chem. Soc.* **1998**, *120*, 7310-7319.
27. Williams, D. H.; Stephens, E.; O'Brien, D. P.; Zhou, M. *Angew. Chem. Int. Ed.* **2004**, *43*, 6596-6616.
28. Sugihara, G.; Shigematsu, D. S.; Nagadome, S.; Lee, S.; Sasaki, Y.; Igimi, H. *Langmuir*, **2000**, *16*, 1825-1833.
29. Bhan, A.; Gounder, R.; Macht, J.; Iglesia, E. *J. Catal.* **2008**, *253*, 221-224.
30. Liu, L.; Guo, Q. X. *Chem. Rev.* **2001**, *101*, 673-695.
31. van der Vegt, N. F.; Trzesniak, D.; Kasumaj, B.; van Gunsteren, W. F. *ChemPhysChem* **2004**, *5*, 144-147.
32. Ford, D. M. *J. Am. Chem. Soc.* **2005**, *127*, 16167-16170.
33. Torres, F. J.; Vitillo, J. G.; Civalleri, B.; Ricchiardi, G.; Zecchina, A. *J. Phys. Chem. C* **2007**, *111*, 2505-2513.
34. Lochan, R. C.; Head-Gordon, M. *Phys. Chem. Chem. Phys.* **2006**, *8*, 1357-1370.
35. Poad, B. L. J.; Wearne, P. J.; Bieske, E. J.; Buchachenko, A. A.; Bennett, D. I. G.; Klos, J.; Alexander, M. H. *J. Chem. Phys.* **2008**, *129*, 184306(1-8).
36. Otero Arean, C.; Turnes Palomino, G.; Garrone, E.; Nachtigallova, D.; Nachtigall, P. *J. Phys. Chem. B* **2006**, *110*, 395-402.
37. Ramirez-Cuesta, A. J.; Mitchell, P. C. H.; Ross, D. K.; Georgiev, P. A.; Anderson, P. A.; Langmi, H. W.; Book, D. *J. Alloys Compd.* **2007**, *446*, 393-396.
38. Ramirez-Cuesta, A. J.; Mitchell, P. C. H.; Ross, D. K.; Georgiev, P. A.; Anderson, P. A.; Langmi, H. W.; Book, D. *J. Mater. Chem.* **2007**, *17*, 2533-2539.
39. Yang, Z.; Xia, Y.; Mokaya, R. *J. Am. Chem. Soc.* **2007**, *129*, 1673-1679.
40. Panella, B.; Hirscher, M.; Roth, S. *Carbon* **2005**, *43*, 2209-2214.
41. Kowalczyk, P.; Holyst, R.; Terrones, M.; Terrones, H. *Phys. Chem. Chem. Phys.* **2007**, *9*, 1786-1792.
42. Wong-Foy, A.G.; Matzger, A.J.; Yaghi, O.M. *J. Am. Chem. Soc.* **2006**, *128*, 3494-3495.
43. Dinca, M.; Yu, A. F.; Long, J. R. *J. Am. Chem. Soc.* **2006**, *128*, 8904-8913.
44. Dinca, M.; Dailly, A.; Liu, Y.; Brown, C. M.; Neuman, D. A., Long, J. R. *J. Am. Chem. Soc.* **2006**, *128*, 16876-16883.
45. Xiao, B.; Wheatley, P. S.; Zhao, X. B.; Fletcher, A. J.; Fox, S.; Rossi, A. G.; Megson, I. L.; Bordiga, S.; Regli, L.; Thomas, K. M.; Morris, R. E. *J. Am. Chem. Soc.* **2007**, *129*, 1203-1209.
46. Forster, P. M.; Eckert, J.; Heiken, B. D.; Parise, J. B.; Yoon, J. W.; Jhung, S. H.; Chang, J. S.; Cheetham, A. K. *J. Am. Chem. Soc.* **2006**, *128*, 16846-16850.
47. Dietzel, P. D. C.; Panella, B.; Hirscher, M.; Blom, R.; Fjellvag, H. *Chem. Commun.* **2006**, 959-961.